

**Few-boson tunneling in a double well with spatially modulated interaction**Budhadyta Chatterjee,<sup>1,\*</sup> Ioannis Brouzos,<sup>2,†</sup> Sascha Zöllner,<sup>3,‡</sup> and Peter Schmelcher<sup>2,§</sup><sup>1</sup>*Physikalisches Institut, Universität Heidelberg, Philosophenweg 12, D-69120 Heidelberg, Germany*<sup>2</sup>*Zentrum für Optische Quantentechnologien, Luruper Chaussee 149, D-22761 Hamburg, Germany*<sup>3</sup>*Niels Bohr International Academy, Niels Bohr Institute, Blegdamsvej 17, DK-2100 København, Denmark*

(Received 22 March 2010; published 22 October 2010)

We study few-boson tunneling in a one-dimensional double well with a spatially modulated interaction. The dynamics changes from Rabi oscillations in the noninteracting case to a highly suppressed tunneling for intermediate coupling strengths followed by a reappearance near the fermionization limit. With extreme interaction inhomogeneity in the regime of strong correlations, we observe tunneling between the higher bands. The dynamics is explained on the basis of the few-body spectrum and stationary eigenstates. For a higher number of particles  $N \geq 3$ , it is shown that the inhomogeneity of the interaction can be tuned to generate tunneling resonances. Finally, a tilted double well and its interplay with the interaction asymmetry are discussed.

DOI: [10.1103/PhysRevA.82.043619](https://doi.org/10.1103/PhysRevA.82.043619)

PACS number(s): 67.85.-d, 67.60.Bc, 03.75.Lm, 05.30.Jp

**I. INTRODUCTION**

Ever since the experimental realization of Bose-Einstein condensation, ultracold atoms have been used to study an enormous diversity of quantum effects with an unprecedented degree of control [1,2]. Advancement in tools, such as optical lattices [3], offer us the chance to explore e.g., second-order tunneling [4], quantum phase transitions [5], and nonequilibrium quantum dynamics of driven systems [6].

The double well especially serves as a prototype system to study interference and tunneling in great detail. For instance, the tunneling dynamics of a Bose-Einstein condensate has been observed to undergo Josephson oscillations [7–9] in which the population simply tunnels back and forth between the two wells. However, when the interaction is raised beyond a critical value, the atoms remain trapped in one well, a nonlinear phenomenon known as self-trapping [7,9,10].

Of special interest are systems in lower dimensions, which often display unique features. Quasi-one-dimensional (1D) Bose gases have been prepared experimentally by freezing the transverse degrees of freedom. There it is possible to tune the interaction strength between the atoms by either using confinement-induced resonances [11] or using magnetic Feshbach resonances [12]. Thus, one can study the crossover from a weakly interacting to a strongly correlated regime. A particularly interesting case is the Tonks-Girardeau gas appearing in 1D in the limit of infinitely repulsive short-ranged interaction, which has been recently observed experimentally [13,14]. This gas of impenetrable bosons is isomorphic with that of free fermions via the Bose-Fermi mapping [15], and all the local properties are identical to the free-fermion system. The gas still retains the bosonic permutation symmetry, and so, the nonlocal quantities differ from the fermionic case.

Theoretically, the quantum dynamics in the weakly interacting case has been studied using the Bose-Hubbard (B-H) model

assuming the validity of a lowest band approximation [16–19]. These studies illuminate relevant tunneling mechanisms and resonances. However, to capture the rich physics present in the stronger interaction regime, we need to go beyond the B-H limit. Moreover, numerically exact calculations of the quantum dynamics for few bosons through a 1D potential barrier [20] or a bosonic Josephson junction [21] reveal deviations from the results obtained with mean-field calculations as well as establish a difference between the dynamics in attractive and repulsive bosonic systems [22]. The crossover from the uncorrelated to the fermionization regime has been investigated for few bosons [23,24] and reveals a transition from Rabi oscillations to fragmented pair tunneling via a highly delayed tunneling process analogous to the self-trapping for condensates. The quantum dynamics of an asymmetric double well while keeping a constant interaction strength has been explored in Refs. [17,18,23,24].

In this investigation, we go one step further and envision a different approach to asymmetry by introducing an inhomogeneous (i.e., spatially varying interaction strength). This can be achieved experimentally by employing magnetic-field gradients in the vicinity of Feshbach resonances or by combining magnetic traps with optically induced Feshbach resonances [12,25]. We will demonstrate how spatially varying interaction strengths enrich the tunneling dynamics in the most fundamental case of a double well. This has to be seen as a potential ingredient for more complex problems, such as quantum transport in optical lattices. Specifically, we study the crossover from the noninteracting to the fermionization limit for a fixed inhomogeneity ratio of interaction and the effect of varying inhomogeneity ratio. An interplay of suppression and resumption of tunneling is observed. For three or more particles, the interaction asymmetry can be tuned to generate various many-particle tunneling resonances. Lastly, we examine a tilted double well and investigate the interplay between the tilt and the inhomogeneity to generate tunneling resonances.

The paper is organized as follows. In Sec. II, we discuss our model and setup. In Sec. III, we briefly describe our computational method. Subsequently, we present and discuss the results for tunneling in a symmetric double well for two

\*bchatter@PHYSnet.uni-hamburg.de

†ibrouzos@PHYSnet.uni-hamburg.de

‡zoellner@nbi.dk

§Peter.Schmelcher@PHYSnet.uni-hamburg.de

atoms first (Sec. IV) followed by more atom systems (Sec. V). In Sec. VI, we discuss the case of an asymmetric double well. Section VII concludes the paper.

## II. SETUP AND INTERACTIONS

Our Hamiltonian (for  $N$  particles) is given by (see Ref. [26] for details)

$$H = \sum_{i=1}^N \left[ \frac{1}{2} p_i^2 + U(x_i) \right] + g \sum_{i < j} \delta(x_i - x_j). \quad (1)$$

The double well  $U(x) = \frac{1}{2}x^2 + h\delta_\omega(x)$  is modeled as a harmonic potential with a central barrier shaped as a Gaussian  $\delta_\omega(x) = \frac{e^{-x^2/2\omega^2}}{\sqrt{2\pi\omega}}$  (of width  $\omega = 0.5$  and height  $h = 8$ , where dimensionless harmonic-oscillator units are employed throughout).

For ultracold atoms, only the  $s$ -wave scattering is relevant, and the effective interaction in 1D can be written as a contact potential [11], which we sample here by a very narrow Gaussian. We focus on repulsive interaction only.

The inhomogeneity of the interaction is modeled as [26]

$$g(R) = g_0 \left[ 1 + \alpha \tanh \left( \frac{R}{L} \right) \right],$$

where  $2R = x_i + x_j$  and  $L$  is the modulation length, which we fix at  $L = 1$ .

For  $R \gg L$ ,  $g$  takes the asymptotic values,

$$g_{\pm} = g_0(1 \pm \alpha).$$

Thus, the parameter  $\alpha$  regulates the relative difference in interaction strength between the left and the right wells,

$$\Delta g \equiv |g_+ - g_-| = 2g_0\alpha,$$

and the corresponding ratio is given by

$$\frac{g_+}{g_-} = \frac{1 + \alpha}{1 - \alpha}.$$

## III. COMPUTATIONAL METHOD

Our goal is to study the bosonic quantum dynamics for weak to strong interactions in a numerically exact fashion. This is computationally challenging and can be achieved only for a few atom systems. Our approach is the multiconfiguration time-dependent Hartree (MCTDH) method [27,28] being a wave-packet dynamical tool known for its outstanding efficiency in high-dimensional applications.

The principal idea is to solve the time-dependent Schrödinger equation,

$$i\dot{\Psi}(t) = H\Psi(t),$$

as an initial value problem by expanding the solution in terms of Hartree products  $\Phi_J \equiv \varphi_{j_1} \otimes \cdots \otimes \varphi_{j_N}$ :

$$\Psi(t) = \sum_J A_J(t) \Phi_J(t). \quad (2)$$

The unknown single-particle functions (SPFs)  $\varphi_j$  ( $j = 1, \dots, n$ , where  $n$  refers to the total number of SPFs used

in the calculation) are, in turn, represented in a fixed primitive basis implemented on a grid. The correct bosonic permutation symmetry is obtained by symmetrization of the expansion coefficient  $A_J$ . Note that in the preceding expansion, not only are the coefficients  $A_J$  time dependent, but also the SPFs  $\varphi_j$ . Using the Dirac-Frenkel variational principle, one can derive the equations of motion for both  $A_J$  and  $\Phi_J$ . Integrating these differential equations of motion gives us the time evolution of the system via Eq. (2). This has the advantage that the basis  $\Phi_J(t)$  is variationally optimal at each time  $t$ . Thus, it can be kept relatively small, rendering the procedure more efficient.

Although MCTDH is designed primarily for time-dependent problems, it is also possible to compute stationary states. For this purpose, the *relaxation* method is used [29]. The key idea is to propagate a wave function  $\Psi_0$  by the nonunitary operator  $e^{-H\tau}$ . As  $\tau \rightarrow \infty$ , this exponentially damps out any contribution but that stemming from the true ground state such as  $e^{-(E_m - E_0)\tau}$ . In practice, one relies upon a more sophisticated scheme called the *improved relaxation* [30,31], which is much more robust especially for excited states. Here,  $\langle \Psi | H | \Psi \rangle$  is minimized with respect to both the coefficients  $A_J$  and the orbitals  $\varphi_j$ . The effective eigenvalue problems thus obtained are then solved iteratively by first solving  $A_J$  with fixed orbital  $\varphi_j$  and then optimizing  $\varphi_j$  by propagating them in imaginary time over a short period. This cycle is then repeated.

## IV. TUNNELING DYNAMICS FOR TWO-BOSON SYSTEM

We first focus on the tunneling dynamics in a symmetric double well with two bosons initially ( $t = 0$ ) prepared in the left well. This is achieved by adding a tilt or a linear potential  $dx$  to the Hamiltonian, hence, making the left well energetically favorable. Instantaneously, the ground state is obtained by applying the relaxation method (imaginary time propagation). For reasonably large  $d$ , this results in achieving a complete population imbalance between the wells. With this state as the initial state, the tilt is instantaneously ramped down ( $d = 0$ ) at  $t = 0$  to study the dynamics in a symmetric double well. Our aim is to study the impact of the correlations between the bosons on the tunneling dynamics both with respect to the interaction strength as well as the spatial inhomogeneity. We start by fixing the inhomogeneity to  $\alpha = 0.2$  (with the left well having lower interaction than the right) and analyze how the dynamics varies with changing interaction strength  $g_0$ .

### A. Dynamics from the uncorrelated to the fermionization limit

In the absence of any interaction  $g_0 = 0$ , the bosons undergo Rabi oscillations between the two wells. This is characterized by complete tunneling of both bosons between the two wells with a single frequency and can be quantified by the time variation of the population of the atoms in the right well,

$$P_R(t) = \langle \Theta(x) \rangle_{\Psi(t)} = \int_0^\infty \rho(x; t) dx,$$

where  $\rho$  is the one-body density. Figure 1 shows that  $P_R$  oscillates sinusoidally between 0 and 1. If we introduce a very small interaction  $g_0 = 0.005$  (inset), the Rabi oscillations

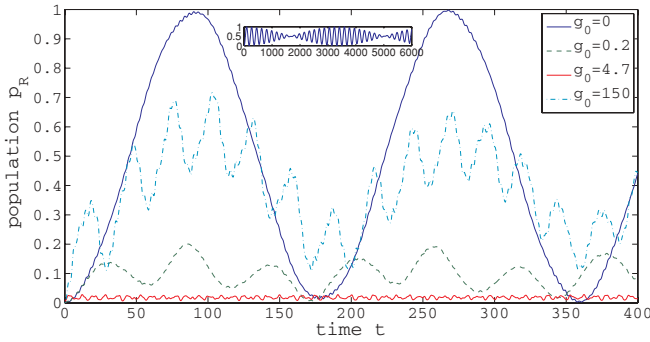


FIG. 1. (Color online) Population of the right-hand well over time  $p_R(t)$  for different interaction strengths at  $\alpha = 0.2$  for two bosons. Inset: Long-time behavior for very low interaction strength  $g_0 = 0.005$ . Barrier height  $h = 8$  and width  $\omega = 0.5$  have been used for all calculations. (All quantities are in dimensionless harmonic oscillator units throughout.)

give way to a beat pattern due to the existence of two very close frequencies. Increasing the interaction strength further ( $g_0 = 0.2$ ), we observe a suppression of tunneling with the maximum population in the right well  $P_R^{\max} \approx 0.2$ . This is a manifestation of the inhomogeneous interaction, which drives the tunneling off-resonance and should be carefully distinguished from the delayed pair tunneling and self-trapping for the same  $g_0$  value in the case of homogeneous interactions (see the following). The dynamics consists of a slow tunneling envelope with suppressed amplitude, which is modulated by a faster oscillation. For higher values of interaction strength ( $g_0 = 4.7$ ), the tunneling is completely suppressed. What remains is a fast oscillation with a tiny amplitude.

However, contrary to the naive intuition, a reappearance of tunneling occurs for larger values of the coupling strength. We observe a partial restoration of tunneling with  $P_R^{\max} = 0.7$  for the value  $g_0 = 150$ , which is close to the so-called fermionization limit. The dynamics is characterized by two frequencies—one very close to the Rabi frequency modulated by a faster oscillation. Ideally, at the fermionization limit  $g_0 \rightarrow \infty$ , the system of hardcore bosons maps to a system of free fermions [15], and all the local properties are identical. Hence, in this limit, we would have complete two-mode single-particle tunneling analogous to tunneling of two free fermions.

Before we move on to analyze the previous observations in detail, let us comment briefly on the differences between the behavior observed in our setup and the case of a symmetric double well with homogeneous interaction. Clearly, both for the non- and infinitely interacting limits, the inhomogeneity does not play a role. For homogeneous interactions and a symmetric trap, tunneling is always resonant and complete. However, different strengths of interaction yield different dynamics, such as a transition from pair tunneling for low interaction strength to a self-trapping mechanism for larger interaction strength, which is characterized by extremely long tunneling times [16,23,24,32,33]. In our case though, we observe an actual suppression of the tunneling amplitude and not so much a delayed process. In the case of an asymmetric well with homogeneous interaction, the effects in the low

interaction regime are equivalent to our setup: The tilt has the same effect as an interaction asymmetry, namely, it destroys resonant behavior thereby leading to a suppression of tunneling [17,18]. Nevertheless, our case is fundamentally different, and this is evident in the strong interaction regime. Specifically, the reemergence of tunneling we observe does not occur in the tilted double-well system.

## B. Analysis

The understanding of the above-described dynamics lies in the variation of the few-body spectrum as  $g_0$  is changed from zero to the fermionization limit [Fig. 2(a)]. Considering the wave function  $\Psi(t) = \sum_m e^{-iE_m t} c_m \Psi_m$  with energy  $E_m$  corresponding to the stationary state  $\Psi_m$ , the population imbalance  $\delta(t) \equiv \langle \Theta(x) - \Theta(-x) \rangle_{\Psi(t)}$  can be computed to be

$$\delta(t) = 4 \sum_{m < n} W_{mn} \cos(\omega_{mn} t) + 2 \sum_m W_{mm} - 1, \quad (3)$$

where  $W_{mn} = \langle \Psi_m | \Theta(x) | \Psi_n \rangle c_m c_n$  and  $\omega_{mn} = E_m - E_n$ .

The energy spectrum of both the noninteracting and the fermionization limit can be understood from the single-particle energy spectrum of the double well, which is in the form of bands each pertaining to a pair of symmetric and antisymmetric orbitals.

In the uncorrelated limit ( $g_0 \rightarrow 0$ ), the low-lying energies of the spectrum are obtained by distributing the atoms over the symmetric and antisymmetric single-particle orbitals in the first band. This leads to  $N + 1$  energy levels,  $N$  being the number of bosons.  $E_m = E_0 + m\Delta^0$  with  $m = 0, \dots, N$  where  $\Delta^0 = \epsilon_1 - \epsilon_0$  is the energy difference between the two single-particle orbitals in the first band. Thus, for  $g_0 = 0$ , the levels are equidistant [Fig. 2(a) inset], and we see Rabi oscillation with frequency  $\omega_{01} = \omega_{12} = \Delta^0$ . As the interaction is increased ( $g_0 = 0.005$ ), this equidistance is slightly broken ( $\omega_{01} \simeq \omega_{12}$ ), and we get a superposition of two very close frequencies. This results in the formation of the beat pattern seen in the dynamics for  $g_0 = 0.005$ .

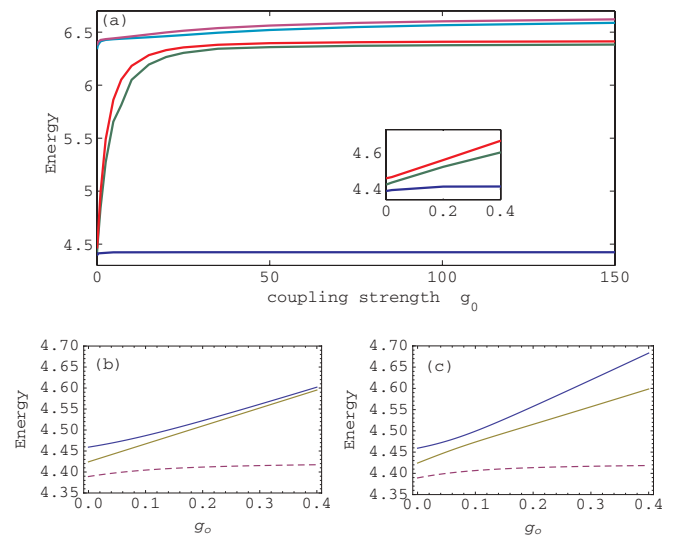


FIG. 2. (Color online) (a) Two-particle energy spectrum as a function of the interaction strength  $g_0$  for  $\alpha = 0.2$ . Inset: Lowest-energy levels for low interaction strength. Bottom: Few-body energy spectrum with  $g_0$  for (b)  $\alpha = 0$  and (c)  $\alpha = 0.2$ .

To understand the dynamics in the low interaction regime, it is instructive to map our system to a two-site B-H Hamiltonian [34,35],

$$\hat{H} = -J(\hat{c}_L^\dagger \hat{c}_R + \hat{c}_R^\dagger \hat{c}_L) + \sum_{j=L,R} \frac{U_j}{2} \hat{n}_j (\hat{n}_j - 1), \quad (4)$$

where  $J$  is the tunneling coupling,  $U_L$  ( $U_R$ ) is the on-site energy of the left (right) well, and  $\hat{n}_j \equiv \hat{c}_j^\dagger \hat{c}_j$ .

Before proceeding, we note here that there is no direct connection between the time-dependent SPF used within our numerical MCTDH calculations and the parameters of the B-H Hamiltonian. In the standard B-H model (which is valid in the weak interaction regime), the parameters  $J$ ,  $U_L$ , and  $U_R$  are time-independent constants, while the shape of the orbitals, such as the localized Wannier functions, retain the shape throughout the course of the dynamics. Moreover, even for low energies, the two most occupied modes for propagation do not necessarily coincide with the two modes of the B-H model. In this weak interaction regime, the B-H model is just a good approximation for our exact calculation, and, thus, we have used it as solely an explanatory tool to analyze the results.

Using the B-H Hamiltonian for  $U_L, U_R \gg J$ , the highest two eigenvalues are approximately  $U_R$  and  $U_L$ . Whereas in the homogeneous case  $\alpha = 0$ , these two levels are close to degenerate  $U_L \approx U_R$  [Fig. 2(b)], here, we have a breaking of the parity symmetry, since  $U_R > U_L$  [Fig. 2(c)]. This is understandable, since the two particles localized in the left well have lower energy than the two particles in the right well leading to the energy level separation seen in Fig. 2(c). In terms of the number-state representation in the localized basis  $|N_L^{(0)}, N_R^{(0)}\rangle$ , the degenerate eigenstates for the homogeneous case read

$$\phi_{1,2} \approx \frac{1}{\sqrt{2}}(|0,2\rangle \pm |2,0\rangle),$$

and, consequently, the dynamics consists of shuffling the probability between the two states corresponding to a complete two-particle tunneling.

In the case of sufficiently strong inhomogeneous interaction, the removal of the degeneracy of the energy levels leads to a decoupling of the eigenstates into localized number states,

$$\phi_1 \approx |2,0\rangle, \quad \phi_2 \approx |0,2\rangle.$$

This implies that the initial state  $\psi(t=0) = |2,0\rangle$  is very close to the first excited state  $\phi_1$  and, thus, is effectively a stationary state of the system. This results in the suppression of tunneling for corresponding values of  $g_0$ .

In the fermionization limit ( $g_0 \rightarrow \infty$ ), the system possesses the same local properties as a system of noninteracting fermions due to the Bose-Fermi mapping [15]. Thus, in an ideal case, the inhomogeneity does not manifest ( $g_{\pm} \rightarrow \infty$ ), and the tunneling dynamics is identical to a system of free fermions. As an idealization, if we consider the initial state as two noninteracting fermions in the left well, then they would occupy the lowest two orbitals localized in the left well. In terms of the single-particle eigenstates of the double well  $|n_{a\beta}^{(\beta)}\rangle$  where  $n_{a\beta}^{(\beta)}$  denotes the occupation number of the symmetric ( $a\beta = 0$ ) or the antisymmetric ( $a\beta = 1$ ) orbital in band  $\beta$ , the

tunneling frequencies  $\omega_{nn'} = E_n - E_{n'}$  are given by [24]

$$\omega_{nn'} = \sum_{\beta} \Delta^{\beta} \underbrace{(n_1^{\beta} - n_1'^{\beta})}_{=0,\pm 1}, \quad (5)$$

where  $\Delta^{\beta}$  denotes the energy splitting of the band  $\beta$  and  $n_1^{\beta}$  represents the occupation of the antisymmetric orbital of the band  $\beta$ . Thus, for two particles, the contributing frequencies are the lowest band Rabi frequency  $\Delta^0$  and the tunnel splitting of the first excited band  $\Delta^1$ . The tunneling dynamics can be pictured roughly as two fermions tunneling independently in the first two bands.

In our system, however, the finiteness of the  $g_0$  value leads to deviations from the ideal fermionic dynamics. The inhomogeneity of the interaction still manifests leading to a difference with respect to the localized two-particle energy level in each well, and the tunneling remains incomplete.

### C. Dynamics with varying inhomogeneity

Having analyzed how the dynamics varies with changing interaction strength at a fixed interaction asymmetry, it is worthwhile to study the dependence of the tunneling dynamics on the strength of the inhomogeneity. For this, we study the effect of different  $\alpha$  values on the tunneling dynamics for a fixed  $g_0 = 0.2$ .

In Fig. 3, we observe that, for  $\alpha = 0$ , we have complete tunneling with a two-mode dynamics [i.e., fast oscillations ( $\omega_{01}$ ), which modulate slower tunneling oscillations ( $\omega_{12}$ )]. When  $\alpha$  is increased to a value of 0.04, the tunneling maximum is reduced to roughly 0.7 while still retaining the two-mode character. As  $\alpha$  is further increased to 0.2, the tunneling is suppressed as described in Sec. IV B. The characteristic display of fast and slow oscillations arising due to the time-scale difference of the contributing frequencies is not prominent here, and, for higher interaction asymmetry ( $\alpha = 0.5$ ), we have effectively single-mode tunneling with frequency  $\omega_{01}$ .

The variation of the maximum population  $P_R^{\max}$  with the inhomogeneity  $\alpha$  (Fig. 3 inset) shows a sharp drop with increasing  $\alpha$  before effectively reaching a constant value  $\sim 0.12$  for  $\alpha \geq 0.3$ . The reader should note that  $P_R^{\max}$  does not go to zero in the asymptotic limit  $\alpha \rightarrow 1$  or  $\frac{U_R}{U_L} \rightarrow \infty$ . This is due to the fact that, with a finite value of  $g_0$  and a finite-barrier

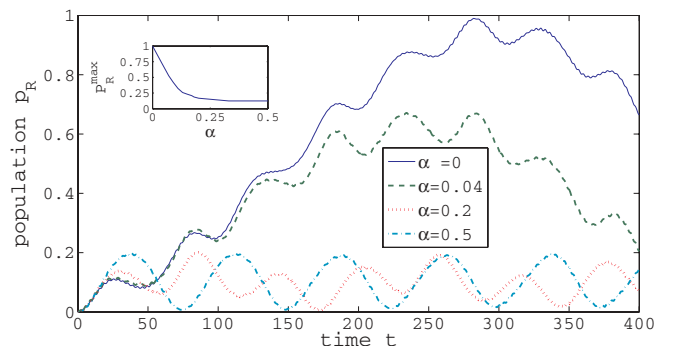


FIG. 3. (Color online) Population of the right well over time  $P_R(t)$  at  $g_0 = 0.2$  for different  $\alpha$  values. Inset: Variation of maximum population of the right well  $P_R^{\max}$  with  $\alpha$  for  $g_0 = 0.2$ .



height, the tunneling coupling ( $J$ ) is not negligible compared to  $U_R$ . As a consequence, there remains a finite probability of bosonic tunneling between the two wells.

#### D. Strong interaction inhomogeneity

An extremely strong inhomogeneity at a high interaction value leads to an interesting higher band tunneling dynamics. We can realize such a system by having  $\alpha = 1$  at  $g_0 = 25$ . This setup effectively makes the bosons fermionized in the right well and almost noninteracting in the left. Preparing the initial setup with both bosons in the left well leads to the suppression of tunneling. However, if we prepare the initial state with two boson in the right well, then we observe substantial tunneling. In Fig. 4(a), we see that the  $P_R$  oscillates between 1 and 0.5 indicating a single-boson tunneling with a single dominant frequency.

In order to understand the phenomenon, we look at the energy spectrum at  $\alpha = 1$  [Fig. 4(b)]. While the ground state remains unaffected, what we see is that, close to the fermionization regime ( $g_0 = 25$ ), the first excited state decouples from the higher three states, which come closer. The main contribution to the first excited state is the state  $|2,0\rangle$ , and its separation from the other states could be understood from the fact that two bosons in the left well are almost noninteracting and, thus, energetically far off-resonant from two effectively fermionized bosons in the right well  $|0,2\rangle$ . The consequences of this fact are the following: (i) The initial configuration of  $|2,0\rangle$  becomes a stationary state resulting in a highly suppressed tunneling, and (ii) the state  $|0,2\rangle$  of the lowest band becomes energetically resonant and couples to the states  $|1^1, 1^0\rangle$  and  $|1^0, 1^1\rangle$  in the higher bands [where the superscripts refer to the ground (0) or the excited (1) orbital of the corresponding well]. The latter leads to a tunneling dynamics in the higher band states predominantly between

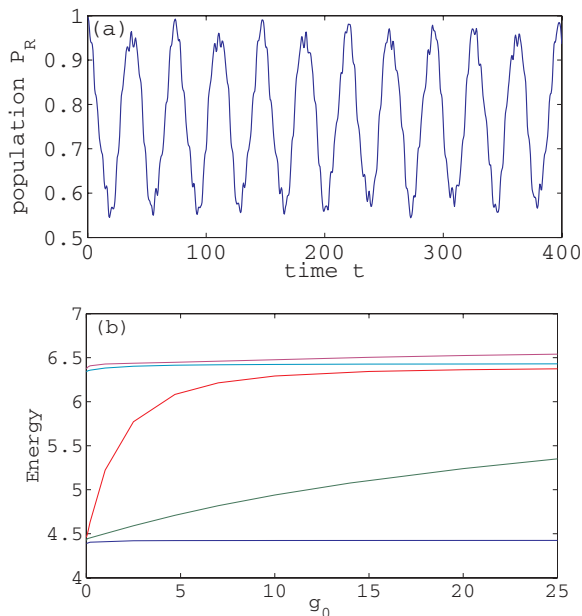


FIG. 4. (Color online) (a) Population variation with time  $P_R(t)$  at  $g_0 = 25$  and  $\alpha = 1$  for  $P_R(0) = 1$  (i.e., initially populating the right well). (b) Energy spectrum for  $\alpha = 1$ .

the second and the fourth excited eigenstates [see Fig. 4(b)], which have greater overlap with the initial state  $|0,2\rangle$ . These orbitals mostly have contributions from the states  $|0,2\rangle$  and  $|1^1, 1^0\rangle$ , while the other orbital has minimal overlap with the initial state. As a result, we get a single-particle tunneling with one dominant frequency given by the splitting of the energy between these two levels. In other words, we effectively have a single-boson tunneling between the wells in the excited band. Note that this highly correlated single-particle tunneling scenario is attributed to the high inhomogeneity in the strong interaction regime, since the combination of these two factors is responsible for turning the pair-tunneling scenario off-resonance.

## V. MULTIPARTICLE DYNAMICS

Having analyzed the tunneling dynamics of two atoms, let us now focus on the case of three or more atoms to see the general atom number dependence of tunneling in the presence of spatially modulated interactions.

#### A. General behavior and mechanisms

Like in the two-boson case, we start with the initial state of  $N = 3$  bosons prepared in the left well. As shown in Fig. 5(a), the main effects are similar to the two-atom case. The dynamics is again governed by frequencies determined by the energy difference of the low-lying spectrum. For very

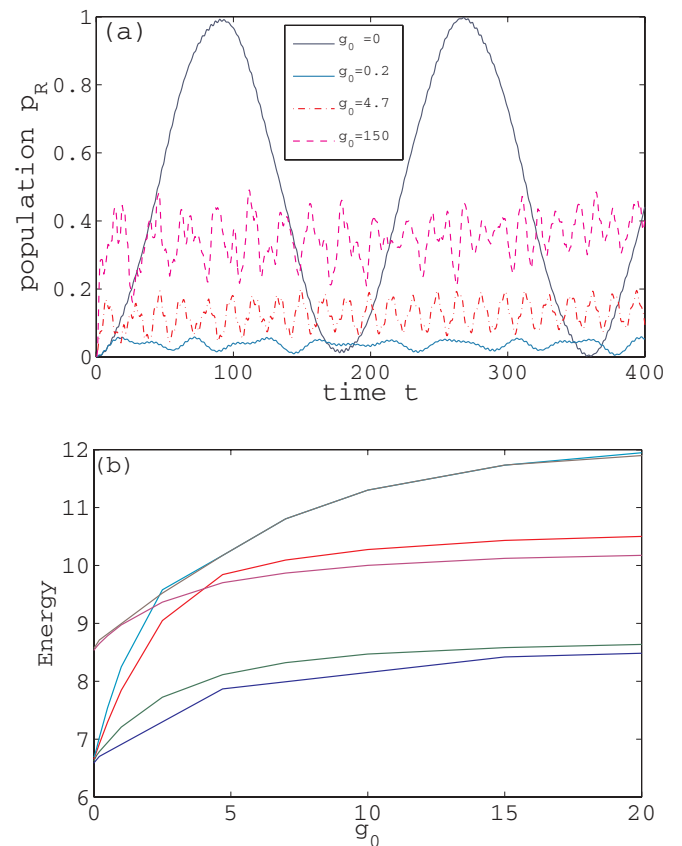


FIG. 5. (Color online) (a) Population of the right-hand well over time  $P_R(t)$ , for three bosons for different interaction strengths at  $\alpha = 0.2$ . (b) Three-boson energy spectrum at  $\alpha = 0.2$ .

small interaction, the nearly equal energy difference gives rise to the beat pattern similar to that of two particles. As we increase the interaction strength, we observe suppression of tunneling for  $g_0 = 0.2$  followed by a partial restoration at  $g_0 = 4.7$  and a higher amplitude reemergence close to the fermionization limit at  $g_0 = 150$ . The general mechanism for the suppression is the same as for the two-particle case. Now, however, in the symmetric case  $\alpha = 0$ , the contributing nearly degenerate eigenstates are of the form  $|N, 0\rangle \pm |0, N\rangle$ . Consequently, we have a complete  $N$ -particle tunneling with a frequency given by [16]  $\omega \sim 2NU/(N-1)!(2\Delta^0/U)^N$  where  $U = U_L, U_R$  denotes the on-site interaction energy. Thus, the tunnel period grows exponentially with  $N$ . When the inhomogeneous interaction is introduced, the states decouple to the localized number states  $|N, 0\rangle$  and  $|0, N\rangle$ , and, thus, the initial state becomes a stationary one leading to the suppression of tunneling. The important thing to note is that with increasing  $N$ , the suppression of tunneling occurs for much smaller values of  $g_0$ . For instance, at  $g_0 = 0.2$  for  $N = 3$ , we have almost complete suppression in contrast with  $N = 2$  where we still observed significant tunneling (see Fig. 1) for this value of  $g_0$ . This could be understood from the fact that the contribution of the on-site energy on the cat state goes as  $\sim U_L(U_R)N(N-1)/2$ , while that of the tunneling term is  $N$  independent. This fact is responsible for a significant decoupling of these states at a lower  $g_0$  value leading to faster suppression of tunneling as  $N$  increases.

Also unlike that of the two-boson case, the spectrum for the three-boson case contains crossings between the higher-lying states [see Fig. 5(b)], and, in the vicinity of these crossings, there is a partial reappearance of tunneling. This can be seen, for instance, at  $g_0 = 4.7$  where we observe a restoration in the three-particle case; whereas for two particles, we still observed a significant suppression (see Fig. 1). In this regime, the higher bands contribute more significantly leading to the convoluted dynamics observed. These higher band contributions lead to further recovery with increasing interaction strength toward the fermionization regime, although even for  $g_0 = 150$ , we do not get the exact fermionic dynamics, which is characterized by the tunneling of three independent fermions.

### B. Generating tunneling resonances by interaction inhomogeneity

A very interesting phenomenon for the  $N \geq 3$  particle case is that, by tuning the asymmetry  $\alpha$ , we get a controllable reemergence of tunneling. To observe this, we study how the tunneling dynamics changes with different values of  $\alpha$  for  $g_0 = 0.2$  (Fig. 6). The value of  $g_0$  is chosen such that the inhomogeneity effect manifests but is still in the two-mode regime. For three atoms, we observe [Fig. 6(a)] that a complete tunneling for  $\alpha = 0$  gives way to suppressed tunneling with increasing  $\alpha$  value. However, at  $\alpha = 0.5$ , we observe a reappearance, which is in the form of a tunneling resonance peaked at  $\alpha = 0.5$  with  $P_R^{\max} \approx 0.6$  corresponding to effective two-boson tunneling. In the case of  $N = 4$ , we see two resonances [Fig. 6(b) inset]—the larger one centered on  $\alpha = 0.3333$  with an amplitude 0.75, and the smaller one centered at  $\alpha = 0.6667$  with an amplitude 0.5 resulting in the reappearance of tunneling shown in Fig. 6(b).

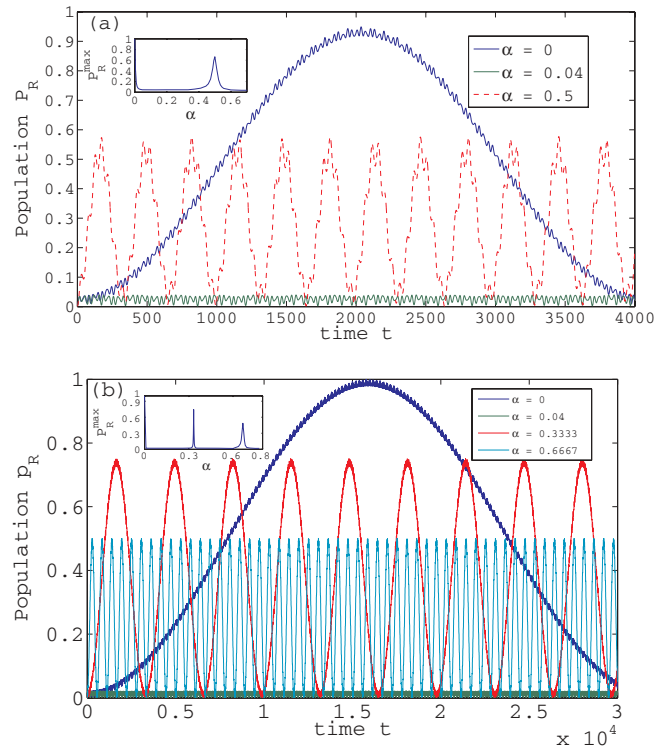


FIG. 6. (Color online) Population of the right well over time  $P_R(t)$  at  $g_0 = 0.2$  for different  $\alpha$  values for (a) three particles and (b) four particles. Inset: Variation of maximum population of the right well  $P_R^{\max}$  with  $\alpha$  for  $g_0 = 0.2$ .

In order to understand this, we have to study the spectra and the underlying eigenstates for different  $\alpha$  (Fig. 7). In the case of  $N = 3$ , for no asymmetry  $\alpha = 0$ , the highest two levels form a doublet [Fig. 7(a)], and the corresponding eigenstates are degenerate of the form  $\frac{1}{\sqrt{2}}(|3, 0\rangle \pm |0, 3\rangle)$ . As  $\alpha$  is increased, the parity symmetry is broken, and the doublets separate, and likewise, the eigenstates decouple [Fig. 7(b)]. The energy eigenvalues (in the limit of very high  $g_0$ ) are given by  $U_L, U_R, 3U_L$ , and  $3U_R$  with the corresponding eigenstates  $|2, 1\rangle, |1, 2\rangle, |3, 0\rangle$ , and  $|0, 3\rangle$ . However, when  $U_R \approx 3U_L$  ( $\alpha = 0.5$ ), the first and the second excited eigenstates become near degenerate and form a doublet of the form  $\frac{1}{\sqrt{2}}(|1, 2\rangle \pm |3, 0\rangle)$  [Fig. 7(c)]. Thus, the initial state  $|3, 0\rangle$  is no longer a stationary state of the system. As a consequence, we get a restoration of tunneling, and the dynamics basically involves shuffling atoms between these two number states. In other words, we have tunneling of two particles between the two wells, while one particle remains in the left well. This resonant two-particle tunneling is what we observe for the  $\alpha = 0.5$  case. As  $\alpha$  is increased further, this degeneracy is once again broken, and the states decouple leading back to the suppressed tunneling dynamics. This is reminiscent of what happens in the asymmetric double well for homogeneous interactions [17].

In a similar consideration, for the four-particle case, the energy eigenvalues are  $3U_L, 6U_L, (U_L + U_R), 3U_R$ , and  $6U_R$ . Now, if  $U_R \rightarrow 2U_L$  ( $\alpha = 0.3333$ ), then we have two degeneracies viz.  $3U_R \rightarrow 6U_L$  and  $(U_L + U_R) \rightarrow 3U_L$  corresponding to the eigenstates  $\frac{1}{\sqrt{2}}(|4, 0\rangle \pm |1, 3\rangle)$  and  $\frac{1}{\sqrt{2}}(|3, 1\rangle \pm |2, 2\rangle)$ . Since the initial state is  $|4, 0\rangle$ , only the first degeneracy

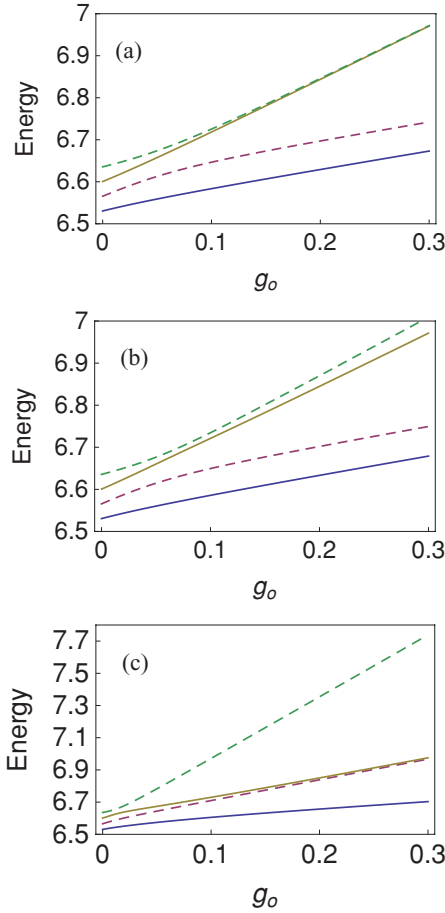


FIG. 7. (Color online) Three-particle energy levels for  $0 < g_0 < 0.3$  for (a)  $\alpha = 0$ , (b)  $\alpha = 0.04$ , and (c)  $\alpha = 0.5$ .

contributes. Thus, the dynamics in this case consists of tunneling of three bosons between the wells, while one boson remains in the left well. This results in the tunneling amplitude of 0.75. The second tunneling peak occurs for  $U_R \rightarrow 5U_L$  ( $\alpha = 0.6667$ ), which leads to  $(U_L + U_R) \rightarrow 6U_L$ . The corresponding degenerate eigenstates are  $\frac{1}{\sqrt{2}}(|4,0\rangle \pm |2,2\rangle)$ , and we observe tunneling of two bosons on top of others remaining in the left well and, thus, the tunneling peak of 0.5. The preceding analysis can be extended generically for  $N$  particles where we would have  $N - 2$  resonances corresponding to the degeneracies between the eigenstates.

### C. Correlations

In order to study the exact nature of tunneling dynamics, we need to investigate the correlations between the particles. For this, we study the temporal evolution of the pair probability or the probability of finding two particles in the same well defined by

$$p_2(t) = \langle \Theta(x_1)\Theta(x_2) + \Theta(-x_1)\Theta(-x_2) \rangle_t, \quad (6)$$

and the three-particle probability or the probability of finding all three particles in the same well defined by

$$p_3(t) = \langle \Theta(x_1)\Theta(x_2)\Theta(x_3) + \Theta(-x_1)\Theta(-x_2)\Theta(-x_3) \rangle_t. \quad (7)$$

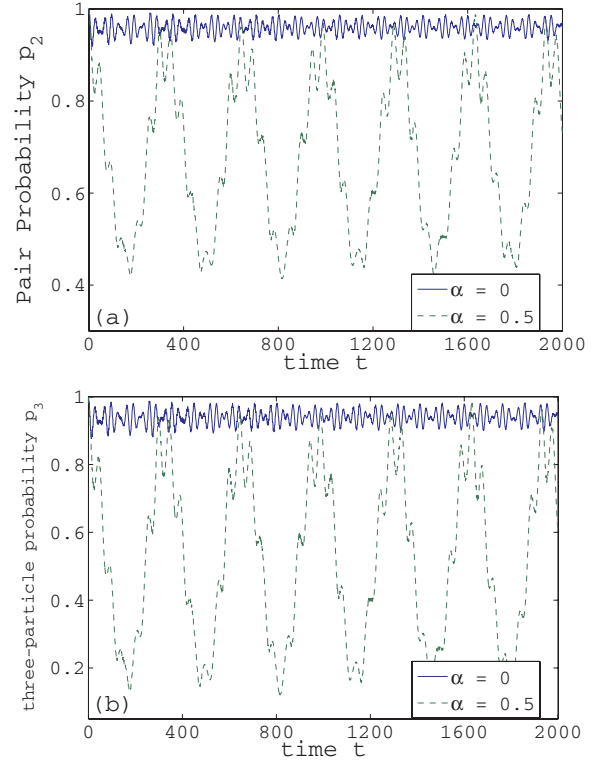


FIG. 8. (Color online) Temporal evolution of (a) pair probability and (b) three-particle probability at  $\alpha = 0$  and  $\alpha = 0.5$  for  $N = 3$  and  $g_0 = 0.2$ .

In the case of  $N = 3$ , for homogeneous interaction  $\alpha = 0$  at  $g_0 = 0.2$ , both  $p_2$  and  $p_3$  oscillate close to unity (Fig. 8). This implies that all three particles can be found in the same well, or, in other words, they tunnel together between the wells. This confirms the analysis of the dynamics by the eigenstate analysis in Sec. IV as tunneling between  $|3,0\rangle$  and  $|0,3\rangle$  states.

Similarly, at resonance ( $\alpha = 0.5$ ), we find that  $p_3$  oscillates from 0.1 and 1 implying that the system oscillates between a three-particle state to a non-three-particle state, namely, the pair state  $|1,2\rangle$ , which can be inferred from the variation of  $p_2$  [Fig. 8(b)]. As a result, we have pair tunneling on top of a particle remaining in the left well. (Ideally, in the case of the B-H model,  $p_2$  should be oscillating between 1 and 0.33, while  $p_3$  should be oscillating between 1 and 0. However, in our case, the realistic potential and parameter regimes as well as some higher band contributions lead to the some deviations from this behavior.)

## VI. ASYMMETRIC DOUBLE WELL

Thus far, we have investigated the dynamics in a symmetric double well with inhomogeneously interacting bosons. An interesting extension is to study the dynamics in an asymmetric double well. This gives us the chance to examine the interplay between the interaction inhomogeneity and the tilt. A special interesting consideration would be to see if the tilt could be tuned to offset the inhomogeneity in the interaction and mimic the dynamics of symmetric interaction

case or further, if it can generate some new tunneling resonances.

**A. Generating tunneling resonances by a tilt**

In symmetric wells with homogeneous interaction, the localized  $N$ -particle state  $|N,0\rangle$  has the same energy as that of the state  $|0,N\rangle$  resulting in a complete  $N$ -particle tunneling between the wells. With the introduction of the inhomogeneity with respect to the interaction, this resonance is broken, and the energy of  $N$  particles in the right well is higher than that in the left well resulting in the suppression of tunneling as seen before. Now, if we incorporate a tilt in the double well such that the left well is lifted and the right well is pushed down energetically in exactly the right amount to make the localized  $N$ -particle energy levels resonant, then we should expect a reemergence of tunneling.

To observe this, we prepare the initial state with both particles in the right well  $\psi(0) = |0,2\rangle$  and study the variation of the tunneling maximum  $P_L^{\max}$  with a tilt  $d$  [Fig. 9(a)] incorporated into the Hamiltonian as a linear term  $-dx$ . We restrict ourselves to the  $\alpha = 0.2$  and  $g_0 = 0.2$  cases. We observe a sharp resonance at  $d \approx 0.0065$  corresponding to the tilt, which exactly balances the localized pair-state energy difference due to inhomogeneous interaction. The result is pair tunneling between the two wells as we would have it in a completely symmetric setup.

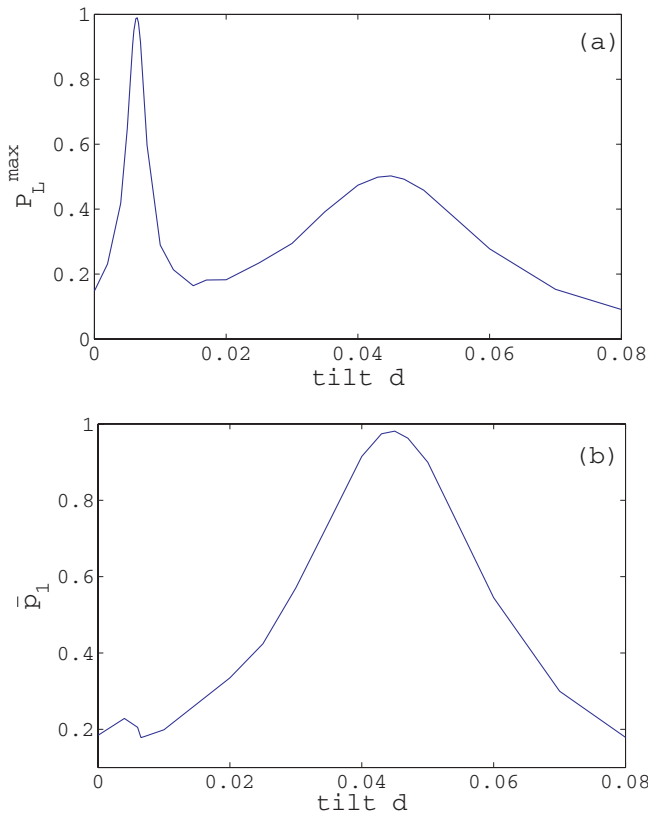


FIG. 9. (Color online) Variation of (a) tunneling maximum  $P_L^{\max}$  with tilt  $d$ , (b) maximum single-particle probability  $\bar{p}_1$  with tilt  $d$  for  $N = 2$ ,  $g_0 = 0.2$ , and  $\alpha = 0.2$ .

With higher tilt, the tunneling maximum falls off very sharply as the pair state becomes off-resonant again, and we get a suppression of tunneling. The next maximum occurs when the tilt is large enough to make the localized pair state  $|0,2\rangle$  resonant with the state  $|1,1\rangle$ . This results in a broad tunneling maximum at  $d \approx 0.045$  corresponding to single-particle tunneling.

To confirm our analysis of the tunneling mechanism, we look at the variation of maximum single-particle probability  $\bar{p}_1$  with tilt [Fig. 9(b)], defined as  $\bar{p}_1 = \max_t [1 - p_2(t)]$ , which gives the probability of having only one particle in a well. We observe a negligible value at the first resonance  $d \approx 0.0065$  confirming that the dynamics is pair tunneling, while a very broad maximum peaked at the second resonance  $d \approx 0.045$  corresponds to the maximum probability of finding a single particle, which in our case is the  $|1,1\rangle$  state, and the dynamics is a single-particle tunneling between the  $|0,2\rangle$  and  $|1,1\rangle$  states.

**B. Spectral analysis**

To understand the effect of the tilt on the tunneling dynamics, we study the energy spectra  $E$  with varying tilt  $d$  at fixed  $g_0 = 0.2$  and  $\alpha = 0.2$  (Fig. 10). At  $d = 0$ , the eigenstates are basically number states in the localized basis. With increasing  $d$ , the highest two levels  $|0,2\rangle$  and  $|2,0\rangle$  move closer and form a sharp avoided crossing at  $d \approx 0.0065$  corresponding to the first tunneling resonance. At this point, the tilt exactly balances the interaction inhomogeneity, and the eigenstate is in the form of the cat state  $|2,0\rangle \pm |0,2\rangle$ . This state is very sensitive to the tilt, and a minute perturbation decouples it into the localized number state resulting in a very sharp tunneling resonance. The ground state, which is the  $|1,1\rangle$  state, is insensitive to the tilt, since this lowering of one particle and raising of another particle keeps the state energetically unaffected within the linear regime. This state forms a broad (anti)crossing with the lower excited state at  $d \approx 0.045$  forming the broad single-particle tunneling resonance seen in the dynamics. This behavior seen in the two-particle case can be expected in general for  $N$  particles giving  $N$  resonances corresponding to the avoided crossings encountered. In particular, with increasing tilt, the successive resonances correspond to a mechanism where one less particle tunnels compared to that of the previous one, while the width of the resonances becomes progressively broader.

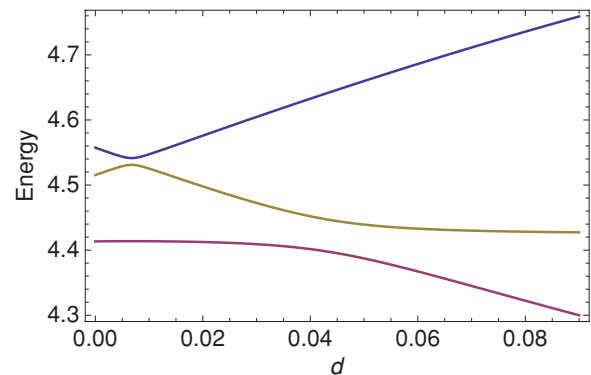


FIG. 10. (Color online) Two-particle energy spectrum with tilt  $d$  for  $\alpha = 0.2$  and  $g_0 = 0.2$ .



## VII. CONCLUSION AND OUTLOOK

We have investigated the double-well tunneling dynamics with inhomogeneous interaction. More specifically, we modeled the system such that we have two different interaction strengths in the two wells. What we observe is that this inhomogeneity leads to a suppression of tunneling. The reason for this suppression can be attributed to the breaking up of the doublet structure in the energy spectrum leading to a decoupling of the eigenstates into the localized number state. Increasing the interaction to the fermionization limit leads to a reappearance of the tunneling. The dynamics is governed by the band splitting of the first two bands, although the finiteness of the interaction strength and the presence of the interaction inhomogeneity lead to deviation from the ideal fermionic behavior. For a very pronounced interaction inhomogeneity for strong interactions, we observe single-particle tunneling between the localized excited bands of the double well.

These basic considerations can be used to understand the many-particle system. There we observed a more severe suppression of tunneling for even lower  $g_0$  values. Most importantly, for  $N \geq 3$  atoms, one can generate tunneling resonances by tuning the interaction asymmetry. These resonances occur as a result of the formation of degeneracies between different eigenstates. For three particles, the exact tunneling mechanism was investigated using the evolution of the pair probability and the three-particle probability. These studies show that we get correlated pair and triplet tunneling with a complete absence of single-particle tunneling.

Finally, we explored the dynamics in an asymmetric double well, and this gives us an understanding of the interplay between the interaction inhomogeneity and the tilt. We observe that the tilt can be tuned to offset the interaction inhomogeneity leading to a tunneling resonance. These dynamics have been explained through the spectral analysis in terms of avoided crossings between the levels. Note that an interesting prospective would be to try to describe the presently found effects in the context of a generalized B-H model, where the on-site energies and the coupling constants would be site and occupation number dependent [36–38].

Understanding the few-body mechanisms of tunneling with spatially modulated interactions can be used to design schemes for selective transport of particles between different wells and/or reservoir systems [39,40]. Furthermore, our study could serve as a starting point for the investigation of the quantum dynamics in the presence of time-dependent interaction modulations and even be extended to multiwell systems [41].

## ACKNOWLEDGMENTS

B.C. gratefully acknowledges the financial and academic support from the International Max-Planck Research School for Quantum Dynamics. Financial support from the German Academy of Science Leopoldina (Grant No. LPDS 2009-11) is gratefully acknowledged by S.Z. P.S. acknowledges financial support by the Deutsche Forschungsgemeinschaft. The authors appreciate fruitful discussions with H. D. Meyer.

- 
- [1] L. Pitaevskii and S. Stringari, *Bose-Einstein Condensation* (Oxford University Press, Oxford, 2003).
  - [2] C. J. Pethick and H. Smith, *Bose-Einstein Condensation in Dilute Gases* (Cambridge University Press, Cambridge, UK, 2008).
  - [3] I. Bloch, J. Dalibard, and W. Zwerger, *Rev. Mod. Phys.* **80**, 885 (2008).
  - [4] S. Fölling *et al.*, *Nature (London)* **448**, 1029 (2007).
  - [5] M. Greiner *et al.*, *Nature (London)* **415**, 39 (2002).
  - [6] E. Kierig, U. Schnorrberger, A. Schietinger, J. Tomkovic, and M. K. Oberthaler, *Phys. Rev. Lett.* **100**, 190405 (2008).
  - [7] M. Albiez, R. Gati, J. Fölling, S. Hunsmann, M. Cristiani, and M. K. Oberthaler, *Phys. Rev. Lett.* **95**, 010402 (2005).
  - [8] G. J. Milburn, J. Corney, E. M. Wright, and D. F. Walls, *Phys. Rev. A* **55**, 4318 (1997).
  - [9] A. Smerzi, S. Fantoni, S. Giovanazzi, and S. R. Shenoy, *Phys. Rev. Lett.* **79**, 4950 (1997).
  - [10] T. Anker, M. Albiez, R. Gati, S. Hunsmann, B. Eiermann, A. Trombettoni, and M. K. Oberthaler, *Phys. Rev. Lett.* **94**, 020403 (2005).
  - [11] M. Olshanii, *Phys. Rev. Lett.* **81**, 938 (1998).
  - [12] T. Köhler, K. Góral, and P. S. Julienne, *Rev. Mod. Phys.* **78**, 1311 (2006).
  - [13] T. Kinoshita, T. Wenger, and D. S. Weiss, *Science* **305**, 1125 (2004).
  - [14] B. Paredes *et al.*, *Nature (London)* **429**, 277 (2004).
  - [15] M. Girardeau, *J. Math. Phys.* **1**, 516 (1960).
  - [16] A. N. Salgueiro *et al.*, *Eur. Phys. J. D* **44**, 537 (2007).
  - [17] L. D. Carr, D. R. Dounas-Frazer and M. A. García-March, *EPL* **90**, 10005 (2010).
  - [18] D. R. Dounas-Frazer, A. M. Hermundstad, and L. D. Carr, *Phys. Rev. Lett.* **99**, 200402 (2007).
  - [19] L. Wang, Y. Hao, and S. Chen, *Eur. Phys. J. D* **48**, 229 (2008).
  - [20] A. U. J. Lode *et al.*, *J. Phys. B* **42**, 044018 (2009).
  - [21] K. Sakmann, A. I. Streltsov, O. E. Alon, and L. S. Cederbaum, *Phys. Rev. Lett.* **103**, 220601 (2009).
  - [22] K. Sakmann, A. I. Streltsov, O. E. Alon, and L. S. Cederbaum, *Phys. Rev. A* **82**, 013620 (2010).
  - [23] S. Zöllner, H.-D. Meyer, and P. Schmelcher, *Phys. Rev. Lett.* **100**, 040401 (2008).
  - [24] S. Zöllner, H.-D. Meyer, and P. Schmelcher, *Phys. Rev. A* **78**, 013621 (2008).
  - [25] D. M. Bauer *et al.*, *Nat Phys.* **5**, 339 (2009).
  - [26] S. Zöllner, H.-D. Meyer, and P. Schmelcher, *Phys. Rev. A* **74**, 053612 (2006).
  - [27] H.-D. Meyer, U. Manthe, and L. S. Cederbaum, *Chem. Phys. Lett.* **165**, 73 (1990).
  - [28] M. H. Beck, A. Jäckle, G. A. Worth, and H.-D. Meyer, *Phys. Rep.* **324**, 1 (2000).
  - [29] R. Kosloff and H. Tal-Ezer, *Chem. Phys. Lett.* **127**, 223 (1986).

- [30] H.-D. Meyer and G. A. Worth, *Theor. Chem. Acc.* **109**, 251 (2003).
- [31] H.-D. Meyer, F. L. Quéré, C. Léonard, and F. Gatti, *Chem. Phys.* **329**, 179 (2006).
- [32] A. P. Tonel, J. Links, and A. Foerster, *J. Phys. A* **38**, 1235 (2005).
- [33] C. E. Creffield, *Phys. Rev. A* **75**, 031607 (2007).
- [34] D. Jaksch, C. Bruder, J. I. Cirac, C. W. Gardiner, and P. Zoller, *Phys. Rev. Lett.* **81**, 3108 (1998).
- [35] M. P. A. Fisher, P. B. Weichman, G. Grinstein, and D. S. Fisher, *Phys. Rev. B* **40**, 546 (1989).
- [36] S. Will *et al.*, *Nature (London)* **465**, 197 (2010).
- [37] P. I. Schneider, S. Grishkevich, and A. Saenz, *Phys. Rev. A* **80**, 013404 (2009).
- [38] K. Sakmann, A. I. Streltsov, O. E. Alon, and L. S. Cederbaum, e-print [arXiv:1006.3530v1](https://arxiv.org/abs/1006.3530v1).
- [39] T. Ernst, T. Paul, and P. Schlagheck, *Phys. Rev. A* **81**, 013631 (2010).
- [40] P. Schlagheck, F. Malet, J. C. Cremon, and S. M. Reimann, *New J. Phys.* **12** 065020 (2010).
- [41] A. I. Streltsov, K. Sakmann, O. E. Alon, and L. S. Cederbaum, e-print [arXiv:0910.5916v1](https://arxiv.org/abs/0910.5916v1).